J. Min. Metall. Sect. B-Metall. 53 (2) B (2017) 139 - 146

Journal of Mining and Metallurgy, Section B: Metallurgy

MICROWAVE-ASSISTED SELECTIVE LEACHING BEHAVIOR OF CALCIUM FROM BASIC OXYGEN FURNACE (BOF) SLAG WITH AMMONIUM CHLORIDE SOLUTION

X. Zhang, G. Ma *, Z. Tong, Z. Xue

The State Key Laboratory of Refractories and Metallurgy, Wuhan University of Science and Technology, Wuhan, China

(Received 02 June 2016; accepted 30 January 2017)

Abstract

The Basic Oxygen Furnace (BOF) slag can be potentially used in the indirect aqueous CO_2 sequestration process due to the fact that it contains large amounts of basic oxides. In this study, microwave-assisted selective leaching of calcium from BOF slag with ammonium chloride solution has been investigated in order to improve the extraction efficiency of calcium ion, and reduce leaching time and the contents of impurity ions in the leachate. The results show that the major phases of BOF slag, such as Ca_2SiO_4, Ca_3SiO_5 and $Ca_2Fe_2O_5$, can react with ammonium chloride solution. The microwave power has significant effects on the leaching ratio of calcium ion from the BOF slag. After microwave-assisted leaching treatment, the internal tiny cracks can be found inside the BOF slag particles. The leaching ratio of calcium ion can be up to 90 % with small amounts of impurity ions existed in the leachate. The non-isothermal leaching reactions are controlled by internal diffusion and the apparent activate energies are estimated to be 6.9-26.5 kJ/mol

Keywords: Microwave; Leaching; Basic Oxygen Furnace slag; Ammonium chloride; CO_2 sequestration

1. Introduction

According to the International Energy Agency, the annual carbon dioxide emissions around the world are ascending year by year, and it had already attained ~3.17×10^{10} t in 2012 [1]. Currently, several measures, such as ocean disposal, geological sequestration and mineral carbonation, can be potentially applied to storage or fix CO_2 [2]. Of these treatment techniques, the concept of mineral carbonation was originally proposed by Seifritz in 1990 [3], and the process routes can be divided into direct and indirect CO_2 sequestration processes. The direct reaction of alkaline mineral particles with gaseous CO_2 was conducted to produce carbonates in the direct CO_2 sequestration process. However, this process was typically carried out at elevated temperature and CO_2 pressure, and the reaction rate of carbonation was very slow [4]. In the indirect CO_2 sequestration process, the calcium or magnesium ion was firstly extracted by acid or salts solutions, and thereafter the leachate was carbonated with CO_2 gas to obtain calcium or magnesium carbonates [5-7]. However, the impurity ions in the leachate were in high concentration in the acid leaching process, and certain amounts of alkaline solvent, such as NaOH, were required to neutralize the acidity in the carbonate stage. The minerals used in the indirect aqueous CO_2 sequestration process mainly include natural Ca/Mg silicates (such as wollastonite and monticellite) and alkaline solid wastes with high Ca/Mg content, such as coal fly ash, construction wastes, steelmaking slag, and so on[7-9].

The steelmaking industry is the third-largest CO_2 emission source in China, and the CO_2 emissions by Chinese steel industry shares 51% of emissions in the world steelmaking industry annually [10]. As a solid by-product of steelmaking process, large quantities of Basic Oxygen Furnace (BOF) steelmaking slag are produced (typically 100-150 kg slag/t steel). Owing to the fact that it is not only near the emission CO_2 facilities, but also rich in basic oxides in BOF slag, especially calcium-containing oxides, it makes BOF slag an excellent material for CO_2 sequestration. The theoretical CO_2 sequestration capacity has been estimated at ~0.25 t CO_2 per tonne slag processed on the basis of the total calcium content in BOF slag [11]. Moreover, the utilization of BOF slag could promote energy saving and emission reduction of steelmaking process, and it is therefore enhance the competitiveness of steel enterprises. Thus, the indirect aqueous carbonation of BOF slag has attracted many attentions recently [12-15]. Kodama et al. [15] developed an indirect mineral carbonation process by using recyclable ammonium chloride as a leaching agent. In this process, the calcium in the BOF slag can be extracted up to ~60% through Eq. 1, and the purity

**Corresponding author: gma@wust.edu.cn*

DOI:10.2298/JMMB160602007Z

of the precipitate calcium carbonate (PCC) products can reach up to 90% with less alkaline solvent consumption due to the requirement for higher pH value of the leachate (more than 9) in the precipitation stage (Eq. 2).

$$4NH_4Cl(a) + 2CaO{\bullet}SiO_2(s) \rightarrow 2CaCl_2(a) + 2SiO_2(s)\downarrow + 4NH_3(a) + 2H_2O(l) \quad (1)$$

$$4NH_3(a) + 2CO_2(a) + 2CaCl_2(a) + 2H_2O(l) \rightarrow 2CaCO_3(s)\downarrow + 4NH_4Cl(a) \quad (2)$$

The slag properties, e.g., the mineralogy and particle size, and leaching process parameters such as the solid to liquid ratio are suggested to strongly influence the calcium extraction efficiency [13-14]. Calcium silicate or lime bound phase as (Ca,Fe,Mn,Mg)O can be the more reactive components for different steelmaking slag [12]. The calcium extraction efficiency from the slag can be improved through lowering the particle size of slag and solid to liquid ratio of the leaching system [14]. The PCC produced from this process is comparable to the PCC produced with conventional methods.

On the other hand, microwave is an electromagnetic wave with the frequency range of 300MHz-300GHz. Since 1980s, microwave-assisted leaching process has been investigated in hydrometallurgical operations to improve the leaching yield of metal ions and shorten the extraction time due to the non-thermal effect of microwave heating which decreases the activation energy of the leaching reactions, the super heating effect which can expand the temperature gradient between solids and liquids and therefore assist the mass transport, as well as the update in the reaction interface for cracks initiated in the mineral particles [16]. Moreover, microwave energy is clean, controllable and environmental friendly.

In this paper, microwave-assisted leaching was applied to selectively extract calcium from BOF steelmaking slag with ammonium chloride solution as a leaching agent. The objective of this paper is to investigate the effects of microwave on the extraction efficiency of calcium with various experimental parameters in order to clarify the kinetics of leaching reactions, and improve the leaching yield to prepare for the high-purity calcium carbonates in the next carbonate stage.

2. Materials and method

2.1 Raw material and its chemical and phase compositions

The BOF slag was collected from a local iron and steel company, it was then ground and dried at 100 °C for 24 h. The chemical composition of the BOF slag was determined with IRIS Advantage ER/S inductively coupled plasma atomic emission spectrometry (ICP-AES). A PHILIPS XL30 TMP scanning electron microscopy with energy dispersive spectrometer (SEM-EDS) was used to examine the microstructure of the BOF slag. The crystalline phases of the slag samples were carried out using an X-ray diffractometer (X'Pert PRO MPD) with Cu Kα radiation at tube voltage of 40KV and current of 40mA. The 2θ scanning ranges are between 10° and 80°.

2.2 Leaching experiments

The analytical reagent grade ammonium chloride (99.5 wt%) was used in the leaching experiment. All the solutions were prepared with deionized water generated from an ultra-pure water purifier (Model QYRO-20A). The microwave-assisted leaching setup was modified with a domestic microwave oven (Model MM721NH1-PW) at a maximum output power of 700 W and a microwave frequency of 2.45 GHz (Fig. 1). The agitator and the sampling glass tube were set at the top of the microwave oven inserted into a 500 ml three-necked flask. The holes were covered by copper wire shield to avoid microwave leakage.

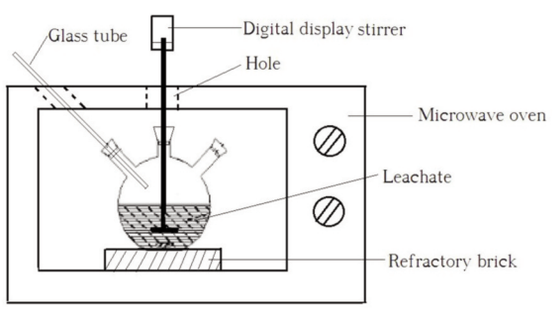

Figure 1. *Microwave-assisted leaching setup*

During the leaching experiment, the BOF slag was mixed with the ammonium chloride solution, and the mixture was put into the three-necked flask placed in the microwave oven. Subsequently, the agitator arm and the glass tube were inserted into the flask. Timing starts when microwave oven was set to work. About 3 mL of leachate sample was collected using a syringe through the glass tube at time intervals of 2, 4, 6, 8, 10, 12, 15 and 20 min. Immediately, same amounts of leaching solution was fed back to the flask after each sampling to avoid the experimental errors. The effects of different experimental parameters, such as microwave output power, solid-to-liquid ratio, stirring speed, concentration of ammonium chloride solution, and volume of leaching agent, on the leaching ratio of calcium ion from the BOF slag were considered in the microwave-assisted leaching test.

Conventional leaching experiment was conducted at 100℃ by using oil bath heating, and the leaching equipment and sampling method were the same as that in microwave-assisted leaching experiment.

2.3. Analitical methods

The collected leachates at certain intervals were filtered and the concentrations of calcium ion and other impurity ions were analyzed with IRIS Advantage ER/S. The leaching ratio of calcium ion (R_{Ca2+}) can be defined as the ratio of total calcium ion content in the leachate to the total calcium content in BOF slag as the following equation

$$R_{Ca2+}=C_{Ca2+}\times V/(W_{slag}\times CaO\%\times 40/56) \quad (3)$$

Where C_{Ca2+} is the concentration of calcium ion in the collected leachates, V is the volume of leaching solution, W_{slag} is the mass of the BOF slag in the leaching experiment, and CaO % is the content of calcium oxide in the BOF slag.

3. Results and discussion

3.1 Chemical and phase compositions of the BOF slag

The chemical composition of BOF slag is shown in Table 1. It is found that the BOF slag contains significant levels of basic oxides, such as CaO (37.71%), Fe_2O_3 (30.42%) and MgO (9.06%), as well as small amounts of SiO_2, Al_2O_3, MnO and P_2O_5. X-ray diffraction (XRD) analysis indicates that the major crystalline phases of the BOF slag are calcium-containing phases, i.e., Ca_2SiO_4, $CaCO_3$, Ca_3SiO_5 and $Ca_2Fe_2O_5$ (Fig. 2). Among the four crystalline phases, $Ca_2Fe_2O_5$ is present as the most abundant phase, and calcite is found possibly due to the carbonation of free lime in the BOF slag.

Table 1. Chemical composition of the BOF slag (wt%)

Oxides	CaO	SiO_2	Al_2O_3	Fe_2O_3	MgO	MnO	P_2O_5
Content	37.71	8.39	2.03	30.42	9.06	2.04	1.21

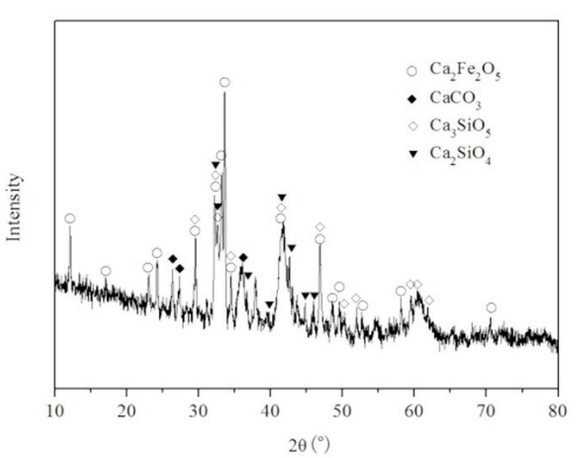

***Figure 2**. XRD pattern of the BOF slag*

3.2 Thermodynamic analysis of leaching reactions

According to the XRD analysis, the standard Gibbs free energies of the leaching reactions between the ammonium chloride solution and the calcium-bearing phases in the BOF slag in the conventional leaching temperature range (0~100°C) were calculated by Factsage 5.3 in order to clarify the possibility of the leaching reactions (Fig. 3). As shown in Fig. 3, the standard Gibbs free energies of leaching reactions between ammonium chloride solution and most of calcium-containing phases in BOF slag, such as $Ca_2Fe_2O_5$, Ca_3SiO_5 and Ca_2SiO_4, are less than 60 kJ/mol, it indicates that these mineral phases could react with ammonium chloride solution in the range of 0 to 100°C [17]. However, the standard Gibbs free energy of leaching reaction between $CaCO_3$ and ammonium chloride solution is considerably more than 60 kJ/mol, which manifests that the reaction between $CaCO_3$ and ammonium chloride solution can not occur in the conventional leaching temperature range [17]. It also indicates that the dissolution reaction of calcium ferrite by ammonium chloride solution can proceed completely for that the standard Gibbs free energy of the reaction ranged between -50~ -100 kJ/mol. Therefore, the leaching reactions of the major phases in the BOF slag and their stoichiometry can be shown as Eqs. 1 and 4:

$$4NH_4Cl(a) + 2CaO\bullet Fe_2O_3(s) \rightarrow 2CaCl_2(a)+2Fe_2O_3(s)\downarrow + 4NH_3(a) + 2H_2O(l) \quad (4)$$

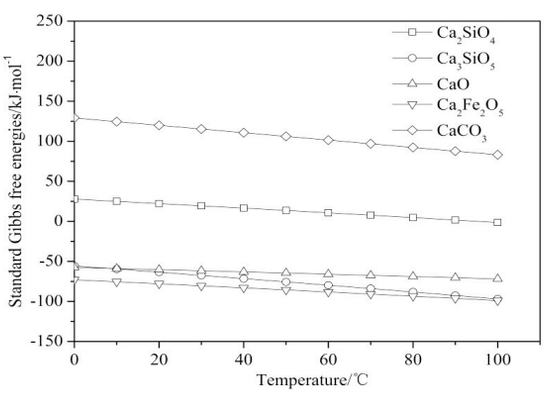

***Figure 3**. The standard Gibbs free energies of leaching reactions with different Ca-bearing phases in the BOF slag*

3.3 Comparison of Ca^{2+} leaching behavior in the microwave-assisted and conventional leaching processes

Fig. 4 shows the leaching behavior of Ca^{2+} from the BOF slag in the microwave-assisted and conventional leaching processes. The leaching experiments were conducted with 300 mL 2 mol/L

ammonium chloride solution, solid-to-liquid (S/L) ratio of 1:20 and stirring speed of 300 rpm. The microwave-assisted leaching experiment was carried out with microwave power of 385 W. It can be found from Fig. 4 that the calcium extraction proceeds very fast at the initial 8 minutes and slow down afterward in the conventional leaching process. According to Tang [18], the leaching reaction of waste slag and ammonium chloride follows shrinking core model, and the reaction is possibly controlled by chemical reaction initially and by diffusion later. In addition, a dense solid product layer forms gradually with the proceeding of leaching reaction and hinders the contact of calcium-containing phases in the core of slag particle with ammonium chloride solution [19]. The leaching ratio of calcium ion from BOF slag can be up to 30.16 % at 20 min in the conventional leaching process. Since the contact area of reactants and the leaching reaction rate constant can be improved in a microwave field, the liquid-solid reaction can be enhanced with intensively migration of ions and/or rotation of dipolar species [20]. The leaching ratio of calcium ion from the BOF slag in the microwave-assisted leaching process improves apparently with the extension of leaching time and reaches up to 57.72 % within 20 min, although the leaching ratio of microwave-assisted leaching process is lower than that of the conventional leaching process within 8 min because the initial leaching temperature of the microwave-assisted leaching system is relatively lower. This indicates that the microwave-assisted leaching process is more efficient than the conventional leaching process due to the heating effect caused by directly volumetric heating and the existence of a non-thermal effect under microwave radiation [16].

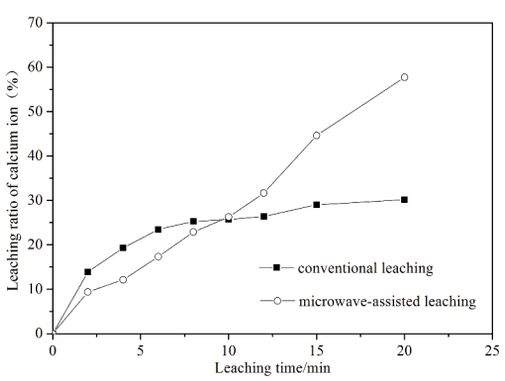

***Figure 4**. Ca^{2+} leaching ratios in the microwave-assisted and conventional leaching processes*

3.4 Effects of microwave power on leaching behavior of Ca^{2+} from the BOF slag

The effects of microwave power on the leaching ratios of Ca^{2+} from BOF slag and temperature profiles of leaching systems measured using a K type thermocouple with shielding device are shown in Fig. 5 and Fig. 6, respectively. Fig. 5 indicates that the improvement of microwave output power results in an increase of leaching ratios of calcium ion in the leachate. This might be due to that leaching system has higher temperature with higher microwave power (as shown in Fig. 6), and the non-thermal effect under microwave radiation is intensified. It is also noted that the leaching ratio of calcium ion can reach up to ~100% with microwave power of 700 W for 20 min. In addition, the temperature rising period to reach the isothermal stage is shortened with an improvement of microwave power.

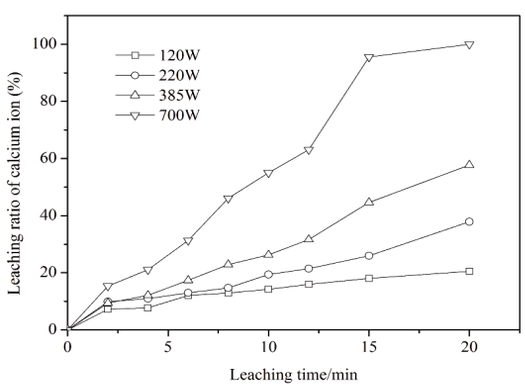

***Figure 5**. Ca^{2+} leaching ratios from the BOF slag with various microwave power (300 ml, 2mol/L NH_4Cl, S/L=1:20, particle size <54μm and 300 rpm)*

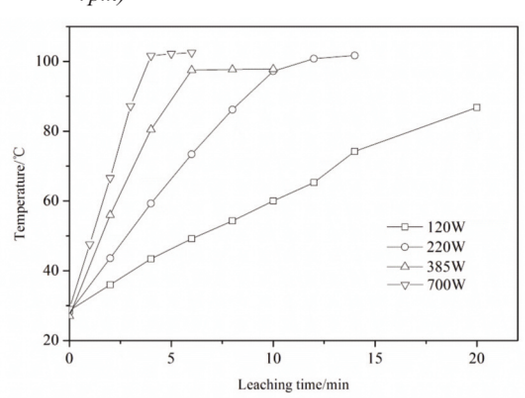

***Figure 6**. Temperature-rising behaviors of leaching system with various microwave power (300 ml, 2mol/L NH_4Cl, S/L=1:20, particle size <54μm and 300 rpm)*

3.5 Effects of solid-to-liquid ratio on leaching behavior of Ca^{2+} from the BOF slag

The influence of different solid-to-liquid ratio on the extraction ratios of Ca^{2+} from BOF slag is shown in Fig. 7. It indicates that the extraction efficiency improves slightly with increasing of solid-to-liquid

ratio, as the improvement of solid-to-liquid ratio brings the relative higher volume of leaching agent corresponding to unit mass of BOF slag, it therefore increases the reaction probabilities between leaching agent and BOF slag particles. In the conventional leaching process, similar leaching behavior of calcium ion is also obtained [13].

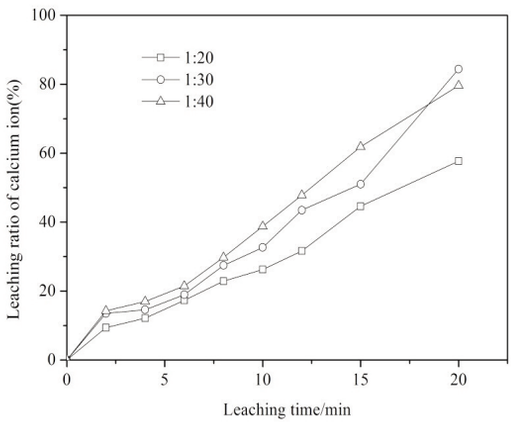

***Figure 7**. Leaching ratios of Ca^{2+} from the BOF slag with different solid-to-liquid ratios (300 mL, 2mol/L NH_4Cl, 385 W, particle size < 54μm and 300 rpm)*

3.6 Effects of concentration of ammonium chloride on leaching ratio of Ca^{2+} from the BOF slag

Fig. 8 illustrates the leaching ratios of calcium ion from BOF slag with different concentrations of ammonium chloride solution in a microwave field. It can be seen that the leaching efficiency of calcium ion improves with the promotion of the concentration of ammonium chloride solution since it causes the increasement of reaction probabilities between BOF slag particles and ammonium chloride. The variations of pH value of leaching systems with different concentrations of ammonium chloride indicates that the initial pH values of leaching systems decrease from 7.93 to 7.59 with the improvement of concentration of ammonium chloride. With the leaching process proceeds, the pH values of each leaching system reduce gradually. However, at the same leaching time intervals, the higher the concentration of ammonium chloride is, the lower the pH value is. The lower pH value of leaching system would benefit for the leaching reactions [21]. However, it has no significant difference on the final leaching ratios of calcium ion with 2mol/L and 4mol/L ammonium chloride in 20 minute. Considering the reduction of the vaporization loss of ammonia owing to the hydrolysis of NH_4^+ in the solution, it is suggested that the concentration of leaching solution may not require too high to avoid the consumption of leaching agent.

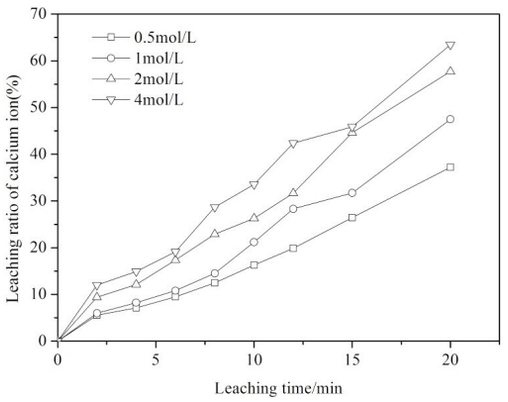

***Figure 8**. Ca^{2+} leaching ratios from the BOF slag with different concentrations of leaching agents (300mL NH_4Cl, S/L=1:20, 385 W, particle size <54μm and 300 rpm)*

3.7 Effects of stirring speed on leaching ratio of Ca^{2+} from the BOF slag

The effect of stirring speed on leaching ratio of Ca^{2+} from the BOF slag is shown in Fig. 9. It indicates that the leaching ratio of Ca^{2+} with different stirring speeds has no significant variation, and this illustrates the external diffusion is possibly not the limiting step of leaching reactions [22].

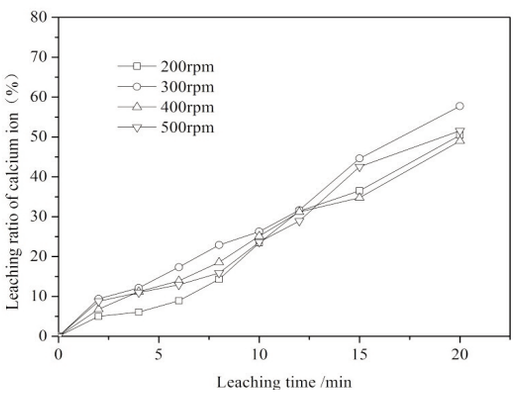

***Figure 9**. Ca^{2+} leaching ratios from the BOF slag with different stirring speeds (300mL, 2mol/L NH_4Cl, S/L=1:20, particle size <54μm and 385 W)*

3.8 Non-isothermal kinetics of leaching process in a microwave field

Leaching process of BOF slag with ammonium chloride solution belongs to the solid-liquid phase reaction. The reactions of calcium-bearing minerals (such as Ca_2SiO_4) in the BOF slag leached by ammonium chloride solution are shown as Eqs. 1 and 4. According to Tong et al. [22], the non-isothermal kinetics equation of microwave-assisted leaching of solid minerals is shown as follows:

$$\ln\{[(1-X)^{1-n}-1]/(n-1)\} = \ln[(Q/\beta_0)\times(E'/R)] \\ -2.315-0.4567[(E'/RT)] \quad (5)$$

where X is the leaching ratio, n is a constant with a value of 2/3, Q is a parameter affected by several factors, such as frequency factor, particle size and concentration of leaching agent, and it can be considered as constant under the condition of these factors remain the same, $\beta_0=e^b$, $E'=E+aR$, R is the gas constant (8.314 J·mol^{-1}·K^{-1}), a and b are both constants related to the microwave power, T is the leaching temperature, and E is the apparent activation energy.

The relationship between the function ln{3[1-(1-X)$^{1/3}$]} and 1/T is linear according to Eq. 5, the slope is -0.4567E'/R, and the Y intercept of line is equal to "ln[(Q/β_0)·(E'/R)]-2.315". In addition, the heating rate of leaching system (β) is not a constant in the non-isothermal stage, and it can be expressed by T as the following Eq. 6.

$$\beta=e^{a/T+b} \quad (6)$$

Thereafter, Eq. 7 can be deduced by taking the logarithm to both sides of Eq. 6.

$$ln\beta=a/T+b \quad (7)$$

By fitting curves to the temperature profiles of Fig. 6, β can be calculated through derivation the temperature-rising curves. The constant a with different microwave powers can be calculated by the slopes and the intercepts of the linear relationship curves between lnβ and 1/T according to Eq. 7. The values of a, b and correlation coefficient r_1 with different microwave powers are shown in Table 2. To test the correlation coefficient r_1 with different microwave powers, the correlation coefficients shown in Table 2 are all bigger than $r^2_{0.05}$=0.95. Thus, lnβ=$a/T+b$ is significant at 0.05 level.

Table 2. *The values of a, b and correlation coefficient r with different microwave powers*

Microwave power/W	120	220	385	700
Constant a	516.3	1349.4	1284.7	1356.6
Constant b	-0.491	-3.007	-1.367	-1.159
Correlation coefficient r_1	0.995	0.98	0.982	0.991

Fig. 10 shows the linear relationship between ln{3[1-(1-X)$^{1/3}$]} and 1/T with different microwave powers at the non-isothermal leaching stage. The apparent activation energies and value of Q with different microwave powers could be obtained by calculating from the values of a in Table 2 and the slopes of fitting curves in Fig. 10. Table 3 shows the apparent activation energies, value of Q and correlation coefficient r_2 with different microwave powers. It can be seen from Table 3 that the correlation coefficient with different microwave powers are all relatively high, and this indicates that the non-isothermal kinetics model is in accordance with the experiment situation. The value of Q increases with the improvement of microwave power within experimental area, meanwhile, the apparent activation energy gradually decreases with an increase of microwave power due to the kinetic compensation effect [23]. It also suggests that the improving of microwave power can promote the leaching reaction. Furthermore, it is suggested that a reaction is chemically controlled when the activation energy is >40 kJ/mol, while the limiting step is physical adsorption/desorption if the activation energy is less than 40 kJ/mol [24]. As the external diffusion is possibly not the limiting step of leaching reactions (Section 3.7), and the values of apparent activation energy with different microwave powers shown in Table 3 are 6.9-26.5 kJ/mol (less than 40 kJ/mol), the limiting step of microwave-assisted leaching of BOF slag in ammonium chloride solution is therefore inner diffusion at non-isothermal leaching stage.

Table 3. *The apparent activation energy, value of Q and correlation coefficient r_2 with different microwave powers*

Microwave power/W	120	220	385	700
Apparent activation energy/kJ·mol^{-1}	26.5	14	10.7	6.9
Value of Q	4.1×10^{-2}	4.5×10^{-3}	6.3×10^{-3}	5.1×10^{-3}
Correlation coefficient r_2	0.994	0.98	0.941	0.973

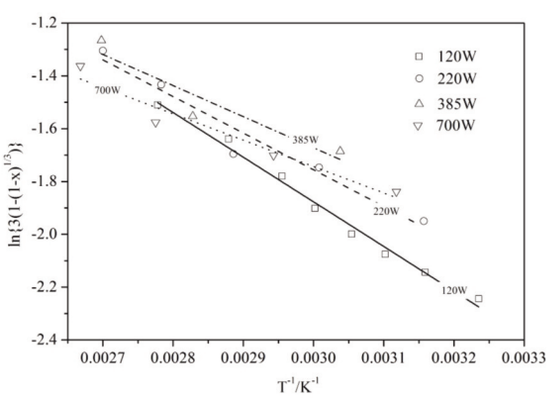

Figure 10*. The relationship between ln{3[1-(1-X)$^{1/3}$]} and 1/T with various microwave powers*

3.9 Leaching behavior of the impurity ions from the BOF slag

The concentrations of major impurity ions (Mg^{2+}, Al^{3+} and Fe^{3+}) in the leaching system (200 mL 2mol/L NH_4Cl, S/L=1:20 and 300 rpm) of the microwave-assisted process with microwave power of 385 W and

the conventional process were measured and shown in Table 4. It can be found from Table 4 that the concentration of Mg^{2+} increases apparently with an increase of leaching time, while the concentrations of Fe^{3+} and Al^{3+} have not varied obviously. Moreover, the relative low concentrations of Fe^{3+} and Al^{3+} will benefit to obtain high purity PCC in the carbonation stage. However, the concentration of Mg^{2+} in the leachate keeps one magnitude lower than that of Ca^{2+}, it still remains at a relative high extraction level. Owing to Mg^{2+} has the same capability of fixation carbon dioxide as Ca^{2+} [25], it will impact the purity of PCC product. As a consequence, Mg^{2+} in the leachate should be controlled further to get high purity PCC product. Compared with the conventional leaching process, it is clear that the concentration of Ca^{2+} is higher in the leachate of microwave-assisted leaching process after 10 mins. Meanwhile, the concentrations of Mg^{2+} of two kinds of leaching processes have little difference, the concentration of Al^{3+} of the microwave-assisted leaching process is significantly lower, while the concentration of Fe^{3+} of microwave-assisted leaching process is higher. This may result from an integration of various effects, mainly including the advantages of microwave heating and the selectively leaching of ammonium chloride solution [26-27].

Table 4. The concentrations of the ions in the leachate of the microwave-assisted leaching (MAL) process and the conventional leaching (CL) process (200mL, 2mol/L NH_4Cl, S/L= 1:20 and 300 rpm)

Leaching time/min	Ca^{2+}/mg·ml^{-1}		Mg^{2+}/mg·ml^{-1}		Al^{3+}/μg·ml^{-1}		Fe^{3+}/μg·ml^{-1}	
	MAL	CL	MAL	CL	MAL	CL	MAL	CL
2	1.18	2.27	0.03	0.14	0.1	1.33	0.48	0.23
4	1.6	2.89	0.06	0.17	0.12	1.33	0.08	0.1
6	2.77	3.38	0.18	0.19	0.1	1.33	4	0.05
8	3.18	3.69	0.23	0.2	0.08	1.75	4.24	0.08
10	4.31	3.67	0.33	0.2	0.02	2.5	6.4	0.03
12	5.06	3.74	0.4	0.2	0.1	1.25	4	0.05
15	7.26	4.22	0.62	0.21	0.06	1.25	3.84	0.05
20	10.52	4.36	1.06	0.21	0.06	2	5.04	0.13

3.10 Characteristics of the residual slag after leaching process

As shown in Fig. 11, the major phases of the residual slag after leaching process (200 mL 2mol/L NH_4Cl, S/L=1:20, 385 W and 300 rpm) are iron oxides, SiO_2, $CaCO_3$ and Ca_2SiO_5. This indicates that most of calcium ferrite minerals and Ca_2SiO_4 in the BOF slag has already reacted with ammonium chloride solution to produce iron oxides and SiO_2. As $CaCO_3$ cannot react with ammonium chloride solution, it remains in the residual slag of leaching process. The presence of Ca_2SiO_4 in residual slag is likely due to that it has not reacted completely with leaching agent within inadequate leaching time. This is consistent with the results of thermodynamic analysis (Fig. 3).

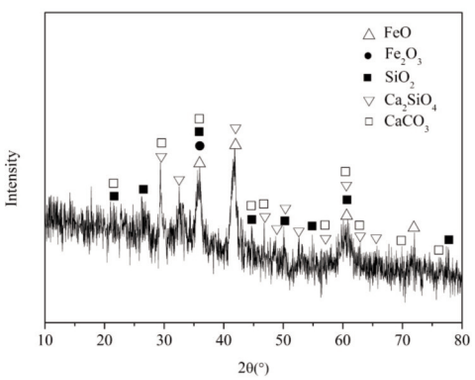

***Figure 11**. XRD pattern of the residual slag after leaching process (200mL, 2 mol/L NH_4Cl, S/L= 1:20, 385 W, particle size < 54μm and 300 rpm)*

The SEM-EDS analysis of the original BOF slag and residual slag after leaching process are shown in Fig. 12. It confirms that the existence of the phases of $CaSiO_4$ and $Ca_2Fe_2O_5$ (Fig. 12a). As the coefficients of thermal expansion and microwave absorbing ability of different crystalline phases in the BOF slag are different, the temperature differences between different phases generated in the microwave-assisted leaching process will result in the local crushing stress and tension stress [28]. The formation of internal tiny

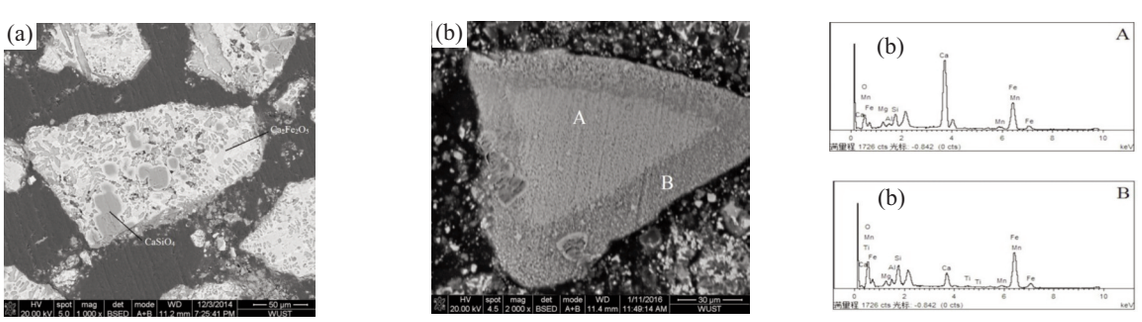

***Figure 12**.SEM-EDS analysis of the original BOF slag (a) and the residual slag after leaching process (b)*

cracks of slag particles increases the effective reaction interface area and therefore promotes the rate of leaching reaction. Furthermore, the SEM-EDS analysis of point B indicates that the unreacted low calcium-bearing phases exist at the out layer of the residual slag particles, this shows that the leaching of BOF slag by ammonium chloride follows shrinking core model (Fig.12b).

4. Conclusions

(1) The major crystalline phases of BOF slag are calcium-bearing minerals. After microwave-assisted leaching process, the internal cracks formed inside the BOF slag particles.

(2) The increase of microwave power, solid-liquid ratio and initial concentration of leaching agent can improve the leaching rate of calcium ion in the leaching process, while the stirring speed has no significant influence on the leaching rate of calcium ion.

(3) In the microwave-assisted leaching process, the apparent activation energy of leaching reactions decreased with microwave power, and the leaching ratio of calcium ion can reach up to 90 % with small amounts of impurity ions existed in the leachate.

(4) The non-isothermal leaching reactions is controlled by internal diffusion and the apparent activate energy is estimated to be 6.9-26.5 kJ/mol.

Acknowledgement

The authors would like to thank the National Nature Science Foundation of China (51374161) and China Postdoctoral Science Foundation (2013M542074) for financial support.

References

[1] IEA, CO_2 emissions from fuel combustion-highlights. International Energy Agency, Paris, 2014, p. 36-38 .

[2] B. Metz, O. Davidson, H. de Coninck, M. Loos, L. Meyer, IPCC special report on carbon dioxide capture and storage, Cambridge University Press, New York, 2005, p. 107-110.

[3] W. Seifritz, Nature. 345 (1990) 486-486.

[4] A. A. Olajire, J. Petrol. Sci. Eng. 109 (2013) 364-392.

[5] S. Teir, H. Revitzer, S. Eloneva, C. J. Fogelholm, R. Zevenhoven, Int. J. Miner. Process. 83 (1) (2007) 36-46.

[6] E. R. Bobicki, Q. Liu, Z. Xu, H. Zeng, Fuel and Energy Abstracts. 38 (2) 2012 302-320.

[7] M. Kakizawa, A. Yamasaki, Y. Yanagisawa, Energy. 26 (01) (2001) 341-354.

[8] O. Capobianco, G. Costa, L. Thuy, E. Magliocco, N. Hartog, R. Baciocchi, Miner. Eng. 59 (5) (2014) 91-100.

[9] M. Verduyn, H. Geerlings, G. van Mossel, S. Vijayakumari, Energy Procedia. 4 (1) (2011) 2885-2892.

[10] IEA and IISI, New comprehensive overview of world industrial energy efficiency and CO_2 intensity. http://www.iea.org/Textbase/press/pressdetail.asp?PRESS-REL-ID=231.

[11] W. J. J. Huijgen, G. Witkamp, R. N. J. Comans, Environ. Sci. Technol. 39 (24) (2005) 9676-82.

[12] S. Eloneva, A. Said, G. J. Fogelholm, R. Zevenhoven,. Appl. Energ. 90 (1) (2012) 329-334.

[13] H. P. Mattila, I. Grigaliunaite, R. Zevenhoven, Chem. Eng. J. 192 (2) (2012) 77-89.

[14] C. Hall, D. J. Large, B. Adderley, H. M. West, Miner. Eng. 65 (6) (2014) 156-162.

[15] S. Kodama, T. Nishimoto, N. Yamamoto, K. Yogo, K. Yamada, Energy. 33 (5) (2008) 776-784.

[16] M. Al-Harahsheh, S. M. Kingman, Hydrometallurgy. 73 (3) (2004) 189-203.

[17] Royal Society of Chemistry, The quantum casino. http://www.presentingscience.com/quantumcasino/index.html.

[18] H. Tang, Study on Fixation of CO_2 by Waste Slags in Steelmaking Plant. Wuhan University of Science and Technology, 2012. (in Chinese)

[19] Y. Sun, M. S. Yao, J. P. Zhang, G. Yang, Chem. Eng. J. 173 (2) (2011) 437-445.

[20] X. Zhai, Q. Wu, Y. F. Yan, L. Ma, C. Fan, N. Li, Trans. Nonferrous Met. Soc. China. 20 (s1) (2010) s77-s81.

[21] Z. Tong, G. Ma, X. Zhang, B. Zhang, Z. Xue, Sep. Sci. Technol. 51 (13) (2016) 2225-2231.

[22] Z. Tong, S. Bi, H. Yu, The Chinese Journal of Nonferrous Metals. 16 (2) (2006) 357-362. (in Chinese)

[23] P. D. Garn, J. Therm. Anal. 10(1) (1976) 99-102.

[24] S. Espiari, F. Raschi, S.K. Sadrnezhaad, Hydrometallurgy. 82 (1-2) (2006) 54-62.

[25] S. Teir, S. Eloneva, C. J. Fogelholm, Energy. 32 (4) (2007) 528-539.

[26] Y. Sun, S. Liu, S. Zhang, J. Zhang, Advanced Materials Research. 581-582 (2012) 1119-1122.

[27] I. S. Pinto, H. M. Soares, Hydrometallurgy, 140 (11) (2013) 20-27.

[28] Y. Chen, N. Yoshikawa, S. Taniguchi, ISIJ Int. 45 (9) (2005) 1232-1237.